

Source Data-Free Cross-Domain Semantic Segmentation: Align, Teach and Propagate

Yuxi Wang, Jian Liang, *Member, IEEE*, and Zhaoxiang Zhang, *Senior Member, IEEE*

Abstract—Benefiting from considerable pixel-level annotations collected from a specific situation (source), the trained semantic segmentation model performs quite well but fails in a new situation (target). To mitigate the domain gap, previous cross-domain semantic segmentation methods always assume the co-existence of source data and target data during domain alignment. However, accessing source data in the real scenario may raise privacy concerns and violate intellectual property. To tackle this problem, we focus on an interesting and challenging cross-domain semantic segmentation task where only the trained source model is provided to the target domain. Specifically, we propose a unified framework called **ATP**, which consists of three schemes, *i.e.*, feature **A**lignment, bidirectional **T**eaching, and information **P**ropagation. First, considering explicit alignment is infeasible due to no source data, we devise a curriculum-style entropy minimization objective to implicitly align the target features with unseen source features via the provided source model. Second, besides positive pseudo labels in vanilla self-training, we introduce negative pseudo labels to this field and develop a bidirectional self-training strategy to enhance the representation learning in the target domain. It is the first work to use negative pseudo labels during self-training for domain adaptation. Finally, the information propagation scheme is employed to further reduce the intra-domain discrepancy within the target domain via pseudo-semi-supervised learning, which is the first step by providing a simple and effective post-process for the domain adaptation field. Furthermore, we also extend the proposed to the more challenging black-box source-model scenario where only the source model’s prediction is available. Extensive results on synthesis-to-real and cross-city driving datasets validate **ATP** yields state-of-the-art performance, even on par with methods that need access to source data.

Index Terms—Domain adaptation, source data-free, feature alignment, negative pseudo labeling, information propagation

1 INTRODUCTION

SEMANITIC segmentation is a fundamental task in the computer vision field that aims to estimate the pixel-level predictions for a given image. Despite the rapid progress on deep learning-based methods, attaining high performance usually demands vast amounts of training data with pixel-level annotations. However, collecting large-scale datasets tends to be prohibitively expensive and time-consuming. Alternatively, previous cross-domain learning approaches [49], [58], [63], [89], [90], [95], [110], [117] attempt to train a satisfactory segmentation model for unlabeled real-world data (called target domain) by exploiting labeled photo-realistic synthetic images (called source domain). However, due to the domain discrepancy, a well-performing model trained on the source domain degrades drastically when it is applied to the target domain. To tackle this issue, various domain alignment strategies are proposed in domain adaptive semantic segmentation field [7], [32], [34], [50], [52], [84], [90].

The essential idea for domain adaptive semantic segmentation is to effectively transfer knowledge from a labeled source domain to a distinct unlabeled target domain. Previous methods achieve this goal by bridging the domain gap in the image level [9], [13], [32], [42], [110], feature level [5], [7], [34], and output level [63], [90], [91], [95].

Although these approaches have made remarkable progress, they usually require access to the labeled source data during the alignment process. However, in some crucial scenarios, the source data is inaccessible due to data protection laws. For instance, the source datasets of autonomous driving and face recognition are unavailable due to data privacy. Thus, this paper addresses a challenging and interesting source data-free domain adaptation issue, where only the trained source model is provided to the target domain for adaptation instead of the source data.

Training a source data-free adaptation model is more challenging than conventional unsupervised domain adaptation approaches. As Figure 1 shows, we describe the difference between traditional unsupervised domain adaptation and source data-free domain adaptation. Due to the absence of source data, previous feature-level alignment or pixel-level alignment methods are not feasible anymore. Moreover, pseudo labels generated from the source-only model are unreliable because of the performance degradation. Besides, we also extend our approach to the black-box source model scenario, where only the predictions of the source model are available, as shown in Figure 1 (c). This problem becomes more challenging but more flexible and practical in the rule of the sever-and-client paradigm. Recent works attempt to address source data-free domain adaptive semantic segmentation by model adaptation [36], [81] or estimating the source data [57]. The approaches highly rely on the prior knowledge of the source model and partially ignore the target-specific information, leading to sub-optimal solutions. Moreover, we are the first to attempt to solve the black-box source model domain adaptive se-

• Y. Wang, J. Liang, and Z. Zhang are with the Center for Research on Intelligent Perception and Computing (CRIPAC), National Laboratory of Pattern Recognition (NLPR), Institute of Automation, Chinese Academy of Sciences (CASIA), and the University of Chinese Academy of Sciences (UCAS), Beijing 100190, China. E-mail: yuxiwang93@gmail.com, liangjian92@gmail.com, zhaoxiang.zhang@ia.ac.cn.
 • Z. Zhang is the corresponding author.

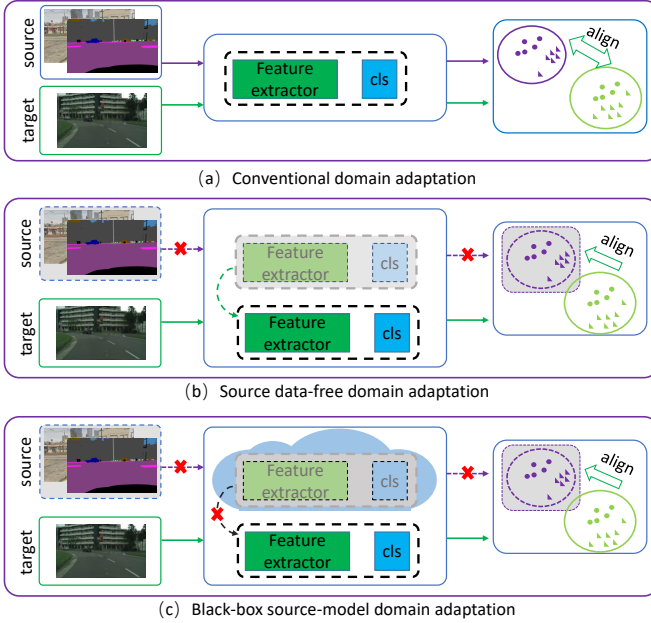


Fig. 1: Comparison between the conventional, source data-free, and black-box source-model domain adaptation for semantic segmentation. The proposed source data-free domain adaptation method only relies on the trained source model, while the conventional methods require all the labeled source data and the target data. Moreover, the black-box model where only the source model's predictions are available can also be leveraged for adaptation.

mantic segmentation in this field.

In this paper, we propose a new framework called **ATP** to tackle source data-free domain adaptive semantic segmentation, which focuses on exploiting the target knowledge to enhance feature representation. Specifically, three pivotal factors are introduced to guide the procedure: implicit feature alignment, bidirectional self-training, and information propagation. Due to the absence of source data, explicit feature alignment approaches are infeasible for source data-free domain adaptation. Consequently, we first provide the implicit feature alignment scheme that aims to ensure the target features are aligned with the source features through hypothesis transfer [53]. Then, considering hard samples perform poorly due to domain discrepancy, explicitly emphasizing these samples at the early training stage may lead to the convergence issue. To address this, we incorporate the idea of Curriculum Learning (CL) [18], [23], [43], [77], [97], [118] into domain adaptation. We develop a curriculum-style entropy loss to emphasize easy samples first and hard samples later automatically. During the bidirectional self-training process, we are among the first to introduce negative pseudo-labeling to the domain adaptation field. Specifically, the negative pseudo labels refer to the predictions with low confidence scores, providing reliable supervised information to indicate the absent classes for corresponding pixels. We further consider vanilla class-balanced [123], [124] positive pseudo labels with high confidence scores and develop a bidirectional self-training strategy to enhance the target representation learning. Fi-

nally, the information propagation scheme aims to reduce intra-domain discrepancy within the target domain because of the different transferability of the target data. Particularly, we conduct a proxy semi-supervised learning task for target data and integrate dominant semi-supervised learning techniques to boost the performance. This propagation acts as a generic simple and effective post-processing module for domain adaptation. Furthermore, we also extend a challenging black-box source model domain adaptation scenario, and the proposed method is spontaneously suitable for this.

The main contributions of this work are summarized as follows.

- 1) We propose a novel source data-free domain adaptation method for semantic segmentation that only requires a trained source model and unlabeled target data. The proposed method can also perform well on the black-box source model scenario, where only the source model's predictions are available.
- 2) We develop a novel curriculum-style entropy objective for implicitly aligning the features of source and target domains.
- 3) We propose a new bidirectional self-training strategy that considers both the positive pseudo labeling and negative pseudo labeling.
- 4) The proposed method yields state-of-the-art cross-domain results on Cityscapes [15] with the semantic segmentation mIoU by 52.6% and 57.9% when adapting from GTA5 [79] and SYNTHIA [80]. Moreover, it performs on par with domain adaptation methods with accessing the source data.

The rest of this paper is organized as follows. Section II gives a brief review for related works about unsupervised domain adaptation, domain adaptive semantic segmentation, source data-free domain adaptation, and semi-supervised learning. Section III presents the detailed procedure of the proposed ATP scheme, including implicit feature alignment, bidirectional self-training, and information propagation. Section IV shows the details, results, analysis, and ablation studies of adaptation experiments in $\text{GTA5} \rightarrow \text{Cityscapes}$, $\text{SYNTHIA} \rightarrow \text{Cityscapes}$, and $\text{Cityscapes} \rightarrow \text{Cross-City}$ [10] tasks. Section V concludes the paper and provides the consideration of the future work.

2 RELATED WORK

2.1 Unsupervised Domain Adaptation

As a typical field of transfer learning [74], unsupervised domain adaptation (UDA) aims to transfer the knowledge from the labeled source domain to a related but distinct unlabeled target domain. Early UDA methods [4], [88], [114] assume the covariate shift with the identical conditional distributions across domains and reduce the domain discrepancy by estimating the weight of each source instance and re-weighting the source empirical risk. Later, researchers [25], [51], [73] resort to domain-invariant feature learning where a common space with the aligned distributions is learned. However, the transferability of these shallow methods is restricted due to the limited representation ability [59].

Recently, deep neural networks approaches have achieved inspiring results for unsupervised domain adaptation in many visual applications, for instance, image classification [27], [61], [96], [98], [119], face recognition [29], [39], objection detection [8], [28], [94], [108], person re-identification [19], [21], [66], [105], and semantic segmentation [49], [63], [72], [90], [95], [99], [116]. The structures of these methods usually have three components: deep feature extractor, task-specific classifier, and domain-invariant feature learning module. Based on the strategies of domain-invariant feature learning, existing deep UDA can be roughly divided into three distinct categories: discrepancy-based, adversarial-based, and reconstruction-based. Discrepancy-based approaches aim to minimize the distance between the source and target distributions by utilizing a divergence criterion. Some favoring choices include maximum mean discrepancy (MMD) [60], high-order central moment discrepancy [115], contrastive domain discrepancy [40], and the Wasserstein metric [20]. As great success has been achieved by GAN method [26], adversarial-based has been a mainstream UDA approach that learns domain-invariant feature representations via confusing source and target domains. DANN [22] adopts a gradient reversal layer (GRL) as a domain-invariant feature learning module, ensuring the feature distributions over two domains are made similar. ADDA [92] provides a symmetrical architecture for source and target mapping, which is flexible to learn a powerful feature extractor. Besides, in contrast to the above binary classifier methods, following works attempt to align joint distribution by considering multiple class-wise domain classifiers [76] or a semantic multi-output classifier [14], [46]. Moreover, reconstruction-based approaches [24] utilize an auxiliary reconstruction task to create a shared domain-invariant representation between two domains and keep the individual characteristic of each domain. In addition, some other reconstruction-based methods [3], [69] further improve the adaptation performance by seeking domain-specific reconstruction and cycle consistency. Beyond them, some other studies also investigate batch normalization [64], [98] and adversarial dropout [47], [83] techniques to ensure feature alignment.

2.2 Domain Adaptive Semantic Segmentation

Domain adaptive semantic segmentation (DASS) is a challenging application for UDA, which aims to provide pixel-level predictions for unlabeled target data. Since Hoffman, *et al.* [33] introduced DASS, it has achieved much attention due to annotating pixel-level labels is labor-expensive and time-consuming. Existing domain adaptation methods for semantic segmentation can be roughly categorized into two groups: adversarial learning based methods and self-supervised learning based methods. For adversarial learning, numerous works focus on reducing the domain discrepancy in the image level, feature level, and output level. Specifically, image-level based methods aim to transfer the domain “style” (appearance) from target to source [106], from source to target [13], [75], [99], [101], [107], or consider both [9], [11], [32], [49], [117], [122]. Feature-level based approaches align distributions between the source and target data at different layers of networks by minimizing the feature discrepancy [120] or adversarial training via a domain

classifier [33], [35], [37]. Output-level adversarial training is first proposed by [90], introducing a discriminator to distinguish the predictions obtained from the source or the target domain. Besides, [95] derives so-called “weighted self-information maps” for minimizing domain discrepancy and [72] diminishes the domain gap by introducing an intra-domain adversarial training process.

For the self-supervised learning method, the essential idea is to generate reliable pseudo labels. Typical approaches usually consist of two steps: 1) generate pseudo labels based on the source model [65], [123], [124] or the learned domain-invariant model [50], [87], [121], 2) refine the target model supervised by the generated pseudo labels [99], [116]. Moreover, [82] and [89] provide a new unaligned score to measure the efficiency of a learned model on a new target domain. Although these methods have achieved promising results, they usually depend heavily on the labeled source data during adaptation. In this paper, we address a challenging source data-free domain adaptation without any raw source data due to the data privacy policy.

2.3 Source Data-free Domain Adaptation

Source data-free domain adaptation is introduced by Chidlovskii *et al.* [12], to tackle domain adaptation problems without accessing the original source dataset. To tackle this problem, [48] exploits the pretrained source model to generate target-style samples, and [1], [53] learns a target-specific feature extraction module by implicitly aligning target representations to the source hypothesis. [45] proposes a universal source data-free domain adaptation when the knowledge of the label space in the target domain is not available. Moreover, a few recent approaches [102], [104], [109] provide model adaptation solutions for classification problems. As for semantic segmentation tasks, model adaptation is also a feasible method to tackle the source data absent setting. Specifically, [57] leverages a generative model to synthesize fake samples to estimate the source distribution and preserve source domain knowledge via knowledge transfer during model adaptation. [81] proposes an uncertainty-reducing method to enhance feature representation. [44] and [111] achieve promising performance via generating a generalized source model trained by data augmentation strategies. In contrast, we offer a simple and effective framework for semantic segmentation tasks, exploiting the target-specific knowledge to intensify the target feature learning. In this paper, we propose a standard three-step framework for domain adaptive semantic segmentation without source data, which includes implicit feature alignment, bidirectional self-training, and information propagation.

2.4 Semi-supervised Semantic Segmentation

Semi-supervised learning (SSL) methods exploit a small number of labeled data and a large amount of unlabeled data during training. The key for semi-supervised learning is to learn a consistent representation between the labeled and unlabeled data. To achieve this goal, recent approaches can be divided into two groups, adversarial-based and consistency-based. Inspired by GAN [26], adversarial-based approaches [38], [67], [86] conduct adversarial loss between

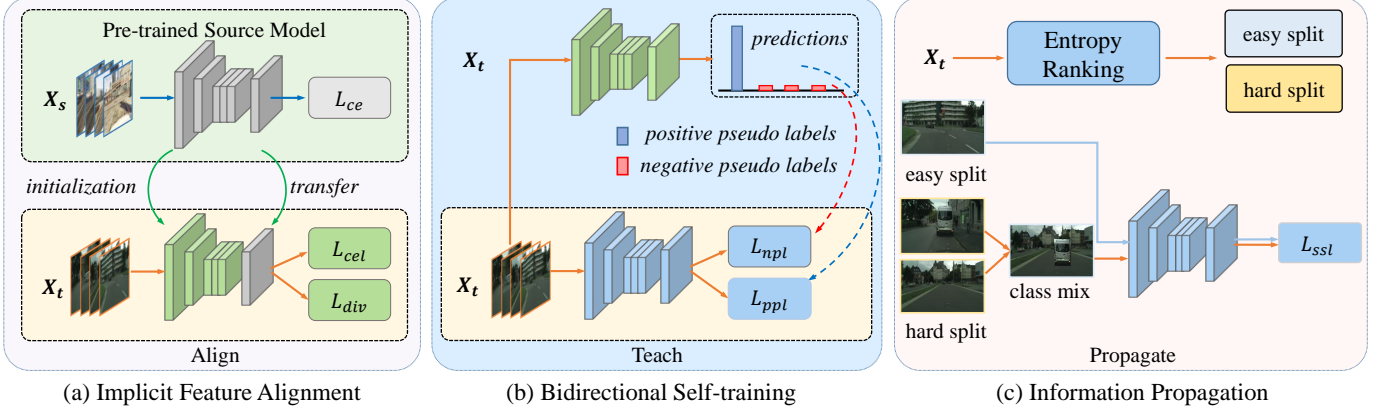


Fig. 2: Illustration of the proposed align, teach, and propagate (ATP) framework for domain adaptive semantic segmentation without source data. (a) is the implicit feature alignment. We freeze the classifier and train the feature extractor to achieve implicit feature alignment by minimizing \mathcal{L}_{cel} and \mathcal{L}_{div} . (b) illustrates the process of bidirectional self-training. Positive and negative pseudo labels are obtained from a fixed model initialized from stage (a). (c) illustrates the process of information propagation. The target data is divided into easy and hard splits according to the entropy ranking, and then we reduce intra-domain discrepancy in a semi-supervised manner by minimizing loss \mathcal{L}_{ssl} .

labeled and unlabeled data. Consistency-based methods [62], [71], [112] utilize data augmentation and consistency regularization to learn feature representation for unlabeled data. Furthermore, [68] first introduces Gaussian perturbations into the input that changes output predictions. Then the strong data augmentation is adopted as solid perturbations. [93] uses the Mixup as the consistency regularization. [103] uses auto-augmentation to generate augmented inputs, and [2] extends the idea by dividing the augmentation set into strong and weak operations. In this work, we refer to the semi-supervised learning strategy to domain adaptation, aiming to reduce the intra-domain discrepancy within the target domain.

3 THE PROPOSED METHOD

In this section, we first introduce the proposed ATP for source data-free domain adaptation, which includes three schemes: the implicit feature alignment, bidirectional self-training, and information propagation. Then we extend the proposed method to a more challenging black-box source model case, where only source model’s predictions are available.

During training, we are given the source model $\mathcal{M}_s : \mathcal{X}_s \rightarrow \mathcal{Y}_s$ trained on n_s labeled images $\{x_s^i, y_s^i\}_{i=1}^{n_s}$ from the source domain \mathcal{D}_s and n_t unlabeled images $\{x_t^i\}_{i=1}^{n_t}$ from the target domain \mathcal{D}_t , where $x_s^i \in \mathcal{X}_s$, $y_s^i \in \mathcal{Y}_s$, and $x_t \in \mathcal{X}_t$. Our goal is to learn a segmentation mapping $\mathcal{M}_t : \mathcal{X}_t \rightarrow \mathcal{Y}_t$ transferring from \mathcal{M}_s , which predicts a pixel-wise label $y_t^i \in \mathcal{Y}_t$ for a given image x_t^i .

The semantic segmentation model \mathcal{M}_s on the source domain is obtained in a supervised manner by minimizing the following cross-entropy loss,

$$\mathcal{L}_{ce} = -\frac{1}{n_s} \sum_{i=1}^{n_s} \sum_{j=1}^{H \times W} \sum_{c=1}^C y_s^{(i,j,c)} \log p_s^{(i,j,c)}, \quad (1)$$

where n_s is the number of source images, H and W denote the image size, and C denotes the number of categories.

$p_s^{(i,j,c)}$ denotes the predicted category probability by \mathcal{M}_s and the $y_s^{(i,j,c)}$ is the corresponding one-hot ground-truth label. Generally, the segmentation model \mathcal{M}_s consists of a feature extractor f_s and a classifier g_s , i.e., $\mathcal{M}_s = f_s \circ g_s$.

To transfer the trained \mathcal{M}_s to the target domain, the proposed ATP framework mainly includes three stages, shown in Figure 2. The implicit feature alignment implicitly enforces the target feature to fit the source model via the proposed curriculum-style entropy minimization and weighted diversity loss, referring to Sec. 3.1. In this stage, the target model is initialized by \mathcal{M}_s and the classifier is frozen during training. Then, we enhance target feature representation learning by the proposed bidirectional self-training technique described in Sec. 3.2, including the positive pseudo labeling and negative pseudo labeling. Finally, we achieve information propagation in a semi-supervised manner, which reduces the intra-domain discrepancy and boosts the adaptation performance with a significant improvement. We will elaborate on the details in the following.

3.1 Implicit Feature Alignment

Without source data, explicit feature alignment that directly minimizes the domain gap between the source and target data can not be implemented. Besides, self-training techniques perform poorly because pseudo labels generated from the source-only model are unreliable. To tackle this problem, we resort to hypothesis transfer and labeling transfer inspired by Liang *et al.* [53]. In contrast, we propose a curriculum-style entropy loss for implicit feature alignment to adapt the source model to the target data. The details will be described in the following.

To eliminate the domain gap, entropy minimization strategy is adopted for training. Although previous methods [72], [95] have demonstrated the effectiveness of entropy minimization, they are not appropriate for the source data-free setting because they treat equal importance for different samples. However, hard-to-transfer samples with uncertain predictions (high entropy values) may deteriorate the

target feature learning procedure. To address this issue, we attempt to explore more reliable supervision from the easy-to-transfer examples with certain predictions (lower entropy values). Inspired by the curriculum learning algorithm [118], [124], we focus the target data training on automatically emphasizing the easy samples first and hard samples later. Specifically, we exploit a curriculum-style entropy loss that expects to rapidly focus the model on certain predictions and down-weight the contribution of uncertain predictions. Formally, the curriculum-style entropy loss is formulated as follows:

$$\mathcal{L}_{cel} = \alpha * (1 - h(x_t))^\gamma * h(x_t), \quad (2)$$

where α balances the importance of certainty/uncertainty predictions and γ controls the weight of certainty samples. $h(x_t) = -\sum_{c=1}^C p_{x_t}^{(h,w,c)} \log p_{x_t}^{(h,w,c)}$ denotes the entropy map and $p_{x_t}^{(h,w,c)}$ is the predicted probability of the target image x_t , i.e., $p_{x_t}^{(h,w,c)} = f_t \circ g_t(x_t)$. f_t and g_t denote the feature extractor and classifier for the target data. Weights of hard-to-transfer samples with higher $h(x_t)$ are reduced and easy samples are emphasized relatively. During training, we pursue hypothesis transfer [53] by fixing classifier module to implicitly align the target features with the source features, i.e., $g_t = g_s$. As we utilize the same classifier module for different domain-specific features, the optimal target features are enforced to fit the source feature distribution as they should have a similar one-hot encoding output. Experiments in Sec. 4 reveal this strategy is important.

From the above loss, the trained model concentrates more on easy-to-transfer classes with a slight domain gap or a large pixel proportion, which may lead to a trivial solution with under-fitting on hard-to-transfer classes. To tackle this issue, we develop a diversity-promoting loss to ensure the global diversity of the target outputs. Exactly, we expect to see the prediction of the target output containing all categories. The proposed confidence-weighted diversity objective is below,

$$\mathcal{L}_{div} = \sum_{c=1}^C \hat{p}_{x_t}^{(h,w,c)} \log \hat{p}_{x_t}^{(h,w,c)}, \quad (3)$$

where $\hat{p}_{x_t}^{(h,w,c)}$ is the weighted mean output embedding of the target image x_t . The weight is calculated based on the entropy $h(x_t)$ and $\hat{p}_{x_t}^{(h,w,c)} = \sum_{(h,w)} \exp(-\lambda * h(x_t)) * p_{x_t}^{(h,w,c)}$. λ is a hyper-parameter and we empirically set $\lambda = 3$ in all experiments. By diversifying the output of target prediction, this technique can circumvent the problem of wrongly predicting confusing target instances as relatively easy classes to learn.

Although the formulation of the proposed curriculum-style entropy loss is similar to focal loss [55], they are entirely different. Specifically, the former is inspired by curriculum learning and it focuses the model adaption on samples from easy to hard. The latter tackles an unbalanced problem by emphasizing hard samples during training.

3.2 Bidirectional Self-training

Previous self-supervised learning methods focus on strengthening the reliability of pseudo labels by developing

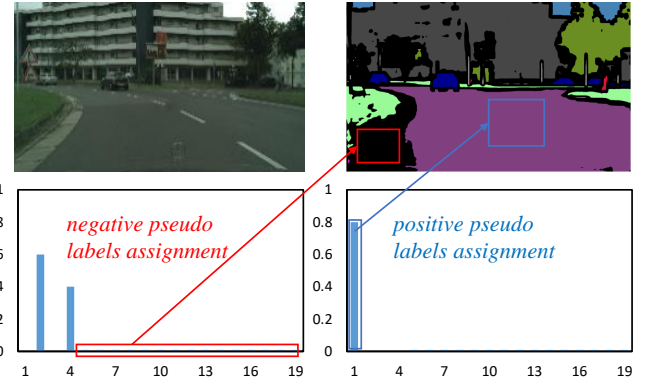


Fig. 3: Bidirectional pseudo labels. Blue refers to positive pseudo labels and red refers to negative pseudo labels.

various denoising strategies [99], [116], but they ignore most of the pixels with lower prediction confidence scores. In that case, the model tends to be over-fitting because the selected over-confident samples lack references using negative pseudo labels. To remedy this, we restrict our attention to the predictions with lower confidence values, termed negative pseudo labels. Although low-confidence predictions cannot be assigned as the correct labels, they will definitely indicate specific absent classes. As Figure 3 shows, it is hard to clearly indicate which category it belongs to for the ignore pixels (black areas), but it is easy to determine which categories it does not belong to. Inspired by this, we propose a bidirectional self-training method that includes positive pseudo labeling and negative pseudo labeling.

Positive pseudo labeling. We first introduce the class-balanced positive pseudo labeling method, which aims to select reliable pseudo labels with high confidence scores for training. Considering the domain-transfer difficulty among different categories, generating pseudo labels according to high confidence will cause hard-to-transfer categories to be ignored. Because easy-to-transfer classes (e.g., roads, buildings, walls, sky) usually have higher prediction confidence scores, while hard-to-transfer classes (e.g., lights, signals, trains, bicycles) perform poorly. Consequently, we assign pseudo-labels based on the guidance of the category-level threshold inspired by [124] as below,

$$\hat{y}_{x_t}^{(h,w,c)} = \begin{cases} 1 & \text{if } c = (\text{argmax}_c p_{x_t}^{(h,w,c)}) \cap (p_{x_t}^{(h,w,c)} > \lambda_c) \\ 0 & \text{otherwise,} \end{cases} \quad (4)$$

where λ_c is a category-level threshold that is determined by the top K predictions within the class c .

Then, we optimize the target model by minimize the categorical cross-entropy with every pseudo label \hat{y}_t :

$$\mathcal{L}_{ppl} = -\frac{1}{n_t} \sum_{i=1}^{n_t} \sum_{j=1}^{H \times W} \sum_{c=1}^C \hat{y}_t^{(i,j,c)} \log p_t^{(i,j,c)}, \quad (5)$$

where n_t is the number of target images, $p_t^{(i,j,c)}$ denotes the predicted category probability, and $\hat{y}_t^{(i,j,c)}$ is the corresponding pseudo label obtained from Eq. (4).

Negative pseudo labeling. For the negative pseudo-label assignment, our goal is to explore the implicit knowl-

edge in uncertainty-aware regions that have been ignored in previous works. Although these predictions have higher uncertainty due to the uniform or low prediction scores, they can definitely point out the absent categories. For example, for a pixel whose output is $[0.48, 0.47, 0.02, 0.03]$, it is impossible to determine which category it belongs to, but we can confidently point out that it does not belong to classes with scores of 0.02 and 0.03. Therefore, we use all absent classes as supervision information for target feature learning. Formally, we assign the negative pseudo labels as follows:

$$\delta(p_{x_t}^{(h,w,c)}) = \begin{cases} 1 & \text{if } p_{x_t}^{(h,w,c)} < \lambda_{neg}, \\ 0 & \text{otherwise,} \end{cases} \quad (6)$$

where λ_{neg} is the negative threshold and we use $\lambda_{neg} = 0.05$ for all experiments. It is worth noticing that the negative pseudo labels are binary multi-labels, which certainly indicates the absence of relative classes. Then the negative pseudo labeling objective is formulated as follows:

$$\mathcal{L}_{npl} = -\frac{1}{n_t} \sum_{i=1}^{n_t} \sum_{j=1}^{H \times W} \sum_{c=1}^C \delta(p_t^{(i,j,c)}) \log(1 - p_t^{(i,j,c)}). \quad (7)$$

Finally, the bidirectional self-training objective includes the positive and negative pseudo labeling:

$$\mathcal{L}_{bst} = \mathcal{L}_{ppl} + \mathcal{L}_{npl}. \quad (8)$$

3.3 Information Propagation

Even we propose a much better solution for global adaptation without source data, intra-domain discrepancy still exists, as previous works [57], [72] indicate. Inspired by the intra-domain alignment method [72], we first divide the target data into easy and hard splits and then close the intra-domain gap to boost the adaptation performance. Contrary to the traditional adversarial mechanism, we borrow a semi-supervised learning scheme by considering the easy split as labeled data and the hard split unlabeled. The target domain is separated using the entropy ranking strategy as below,

$$r(x_t) = \frac{1}{HW} \sum_{h=1}^H \sum_{w=1}^W h(x_t)^{(h,w)}, \quad (9)$$

which is the mean entropy for a target image x_t with the corresponding entropy map $h(x_t)$. Easy and hard splits are conducted from the ranking of $r(x_t)$ following $ratio = \frac{\|x_{te}\|}{(\|x_{te}\| + \|x_{th}\|)}$, where x_{te} and x_{th} denote the easy split and the hard split, respectively.

After that, we conduct a proxy semi-supervised learning task based on the assumption that it is necessary to mitigate intra-domain discrepancy and pseudo labels of the easy part are reliable. We borrow semi-supervised learning techniques to bridge the intra-domain gap. We incorporate dominant semi-supervised learning approaches, including consistency-based methods [70], [103] and contrastive learning methods [56], and propose the following propagation objective:

$$\begin{aligned} \mathcal{L}_{ssl} = & \mathcal{L}_{ce}(\mathcal{M}_t(x_{te}), \hat{y}_{te}) + \\ & \mathcal{L}_{cyc}(\mathcal{M}_t(\mathbf{Aug}(x_{th})), \mathcal{M}'_t(x_{th})), \end{aligned} \quad (10)$$

Algorithm 1: ATP

Data: training dataset: \mathcal{X}_t ; the trained source model: \mathcal{M}_s ; parameters: α , γ , λ_c , and λ_{neg} ;
Result: the output target model \mathcal{M}_t

```

1 Warmup:  $\mathcal{M}_s \leftarrow (\mathcal{X}_s, \mathcal{Y}_s)$  according to Eq.(1), which
   is trained before;
2 Align:
3 initialization:  $\mathcal{M}_{t_0} = f_{t_0} \circ g_{t_0} \leftarrow \mathcal{M}_s$ .  $f_{t_0}$  is
   optimized and  $g_{t_0}$  is frozen.
4 for  $m \leftarrow 0$  to  $epochs$  do
5   | Optimize  $\mathcal{M}_{t_0}$  by minimizing the proposed
     losses  $\mathcal{L}_{cel}$  Eq. (2) and  $\mathcal{L}_{div}$  Eq. (3);
6 end
7 Teach:
8 initialization:  $\mathcal{M}_{t_1} \leftarrow \mathcal{M}_{t_0}$ ;
9  $\mathcal{P}$  is a set of positive prediction samples;  $\mathcal{N}$  is a set
   of negative prediction samples;
10 for  $stage \leftarrow 1$  to  $S$  do
11   | Generate positive pseudo labels set
      $\mathcal{P} \leftarrow \mathcal{M}_{t_1}(\mathcal{X}_t; \lambda_c)$  according to Eq. (4);
12   | for  $m \leftarrow 0$  to  $epochs$  do
13     |   | Get negative pseudo labels
          $\mathcal{N} \leftarrow \mathcal{M}_{t_1}(\mathcal{X}_t; \lambda_{neg})$  according to Eq. (6);
14     |   | Train model  $\mathcal{M}_{t_1}$  using the proposed
         |   | bidirectional self-training technique
         |   | according to Eq. (8);
15   | end
16 end
17 Propagate:
18 initialization:  $\mathcal{M}_t \leftarrow \mathcal{M}_{t_1}$ ;
19 Divide the target data  $\mathcal{X}_t$  into easy split  $\mathcal{X}_{te}$  and
   hard split  $\mathcal{X}_{th}$  according to Eq. (9);
20 Generate pseudo labels  $\hat{y}_{te}$  for easy split  $\mathcal{X}_{te}$ ;
21 for  $m \leftarrow 0$  to  $epochs$  do
22   | Apply data augmentation for the hard target
     | data  $\mathbf{Aug}(x_{th})$ ;
23   | Optimize  $\mathcal{M}_t$  by minimizing the proposed loss
     |  $\mathcal{L}_{ssl}$  according to Eq. (10);
24 end
25 Return  $\mathcal{M}_t$ 

```

where \hat{y}_{te} denotes the pseudo labels of x_{te} obtained from the trained model in Eq. (8). \mathcal{L}_{ce} is the cross-entropy loss and \mathcal{L}_{cyc} is the consistency loss [103]. $\mathbf{Aug}(x)$ denotes data augmentation operation for image x . \mathcal{M}'_t offers the values of target model \mathcal{M}_t without gradient optimization.

Unlike the most closely related work [72] that reduces intra-domain gap by conducting intra-domain adversarial learning, our work directly learns consistency representations for the target data in a semi-supervised learning manner. Notice that the adopted technique can be considered as a standard post-process for adaptation, which is more simple and stable than the adversarial learning method.

3.4 Extension for Black-Box Source Model

In this section, we extend our method to the challenging black-box source model case [54], where only the target data and the corresponding predictions of the source model are available. It is a more practical scenario because we

TABLE 1: Results of GTA5 → Cityscapes (CS). “SF” denotes the source data-free setting. **Red** is the best result for source data-free methods. **Blue** is the best for source data-dependent methods.

Method	SF	road	side.	build.	wall	fence	pole	light	sign	vege.	terr.	sky	person	rider	car	truck	bus	train	motor.	bike	mIoU
AdaptSeg [90]		86.5	36.0	79.9	23.4	23.3	23.9	35.2	14.8	83.4	33.3	75.6	58.5	27.6	73.7	32.5	35.4	3.9	30.1	28.1	42.4
ADVENT [95]		89.4	33.1	81.0	26.6	26.8	27.2	33.5	24.7	83.9	36.7	78.8	58.7	30.5	84.8	38.5	44.5	1.7	31.6	32.4	45.5
CBST [124]		91.8	53.5	80.5	32.7	21.0	34.0	28.9	20.4	83.9	34.2	80.9	53.1	24.0	82.7	30.3	35.9	16.0	25.9	42.8	45.9
MaxSquare [7]	✗	89.4	43.0	82.1	30.5	21.3	30.3	34.7	24.0	85.3	39.4	78.2	63.0	22.9	84.6	36.4	43.0	5.5	34.7	33.5	46.4
CAG_UDA [117]	✗	90.4	51.6	83.8	34.2	27.8	38.4	25.3	48.4	85.4	38.2	78.1	58.6	34.6	84.7	21.9	42.7	41.1	29.3	37.2	50.2
FDA [110]		92.5	53.3	82.4	26.5	27.6	36.4	40.6	38.9	82.3	39.8	78.0	62.6	34.4	84.9	34.1	53.1	16.9	27.7	46.4	50.5
PLCA [41]		84.0	30.4	82.4	35.3	24.8	32.2	36.8	24.5	85.5	37.2	78.6	66.9	32.8	85.5	40.4	48.0	8.8	29.8	41.8	47.7
SIM [100]		90.6	44.7	84.8	34.3	28.7	31.6	35.0	37.6	84.7	43.3	85.3	57.0	31.5	83.8	42.6	48.5	1.9	30.4	39.0	49.2
SFDA [57]		84.2	39.2	82.7	27.5	22.1	25.9	31.1	21.9	82.4	30.5	85.3	58.7	22.1	80.0	33.1	31.5	3.6	27.8	30.6	43.2
URMA [81]		92.3	55.2	81.6	30.8	18.8	37.1	17.7	12.1	84.2	35.9	83.8	57.7	24.1	81.7	27.5	44.3	6.9	24.1	40.4	45.1
S4T [78]	✓	89.7	39.2	84.4	25.7	29.0	39.5	45.1	36.8	86.8	41.8	79.3	61.2	26.7	85.0	19.3	28.2	5.3	11.8	9.3	44.8
SFUDA [111]		95.2	40.6	85.2	30.6	26.1	35.8	34.7	32.8	85.3	41.7	79.5	61.0	28.2	86.5	41.2	45.3	15.6	33.1	40.0	49.4
HCL [36]		92.0	55.0	80.4	33.5	24.6	37.1	35.1	28.8	83.0	37.6	82.3	59.4	27.6	83.6	32.3	36.6	14.1	28.7	43.0	48.1
ATP (w/o TP)		90.1	33.7	83.7	31.5	20.6	31.7	34.5	25.4	84.8	38.2	82.0	59.9	26.9	84.5	25.9	38.9	6.9	23.8	32.1	45.0
ATP (w/o P)	✓	90.4	43.9	85.1	40.4	23.8	34.2	41.8	34.3	84.2	35.9	85.5	62.3	21.9	83.8	36.9	51.8	0.0	36.8	53.0	49.8
ATP		93.2	55.8	86.5	45.2	27.3	36.6	42.8	37.9	86.0	43.1	87.9	63.5	15.3	85.5	41.2	55.7	0.0	38.1	57.4	52.6

can utilize all kinds of server API as our source model. As no parameters are available, the source model can be treated as a black box, only providing the predictions of the target data. Due to no access to the trained source model parameters, the implicit feature alignment is impractical. Alternatively, a natural knowledge distillation (KD) [31] method is adopted to transfer the soft predictions from the source model to the target model. In this case, we pursue the knowledge distill to enforce the target model performing a similarity prediction with the source model. The knowledge distillation loss is formulated as follows:

$$\mathcal{L}_{kd} = \mathbb{E}_{x_t \in \mathcal{X}_t} \mathcal{D}_{kl}(f_s \circ g_s(x_t); f_t \circ g_t(x_t)), \quad (11)$$

where \mathcal{D}_{kl} denotes the Kullback-Leibler divergence loss. After that, we apply our bidirectional self-training strategy and information propagation based on the target student model.

3.5 Algorithm

In this section, we provide the algorithm of **ATP** in Algorithm 1, which consists of three stages, *Align*, *Teach*, and *Propagate*. The first stage refers to the *implicit feature alignment*, which enforces the target feature representations fitting to the source model. In the second stage, we use *bidirectional self-training* strategy that contains the positive pseudo labeling and the negative pseudo labeling to enhance the feature representation learning. The third stage is related to the *information propagation*, which reduces intra-domain discrepancy in a semi-supervised learning manner.

4 EXPERIMENTS

4.1 Datasets

We demonstrate the efficacy of the proposed method on the standard adaptation tasks of GTA5 [79] → Cityscapes [15], SYNTHIA [80] → Cityscapes and Cityscapes → NTHU Cross-City [10]. The synthetic dataset **GTA5** contains 24,966

annotated images with a resolution of 1914×1052 , token from the famous game Grand Theft Auto. The ground truth is generated by the game rendering itself. **SYNTHIA** is another synthetic dataset, which contains 9,400 fully annotated images with the resolution of 1280×760 . **Cityscapes** consists 2,975 annotated training images, and 500 validation images with the resolution of 2048×1024 . **NTHU Cross-City** dataset has been recorded in four cities: Rome, Rio, Tokyo, and Taipei. Each city set has 3,200 unlabeled training images and 100 testing images with the resolution of 2048×1024 . We employ the mean Intersection over Union (mIoU) as the evaluation metric which is widely adopted in semantic segmentation tasks.

4.2 Implementation Details

We use the DeepLab [6] architecture with ResNet-101 [30] pre-trained on ImageNet [16] as the backbone, which is the same as previous works [63], [90], [95]. We first pre-train the segmentation network on the source domain for 80k iterations to obtain a high-quality source model. Then it is considered as the initialization model. During training, we follow previous works [63], [90], [95] using Stochastic Gradient Descent (SGD) optimizer with the learning rate 2.5×10^{-4} , momentum 0.9, and weight decay 5×10^{-4} . We schedule the learning rate using “poly” policy: the learning rate is multiplied by $(1 - \frac{\text{iter}}{\text{max_iter}})^{0.9}$. In the entropy minimization stage, we fix the classifier as above mentioned. In the other stages, the classifier is optimized with the learning rate 2.5×10^{-3} . Concerning parameters, we follow unsupervised hyper-parameters selection method [82] to tune the following parameters. We first freeze γ and choose $\alpha = 0.002$ from the range of [0.001, 0.002, 0.003], and then the value of γ is selected as 3 from the range of [0, 1, 2, 3, 4, 5]. For self-training process, we assign the threshold λ_c according to the category-level top $K = 65\%$ target predictions to generate pseudo-labels, and the threshold of negative pseudo labels λ_{neg} is assigned as 0.05. We update pseudo labels epoch by epoch, and the maximum number of epochs

TABLE 2: Results of SYNTHIA → Cityscapes. “SF” denotes the source data-free setting. **Red** is the best result for source data-free methods. **Blue** is the best result for source data-dependent methods.

Method	SF	road	side.	build.	wall*	fence*	pole*	light	sign	vege.	sky	person	rider	car	bus	motor.	bike	mIoU*	mIoU
AdaptSeg [90]		79.2	37.2	78.8	-	-	-	9.9	10.5	78.2	80.5	53.5	19.6	67.0	29.5	21.6	31.3	-	45.9
ADVENT [95]		85.6	42.2	79.7	8.7	0.4	25.9	5.4	8.1	80.4	84.1	57.9	23.8	73.3	36.4	14.2	33.0	41.2	48.0
CBST [124]		68.0	29.9	76.3	10.8	1.4	33.9	22.8	29.5	77.6	78.3	60.6	28.3	81.6	23.5	18.8	39.8	42.6	48.9
MaxSquare [7]	✗	82.9	40.7	80.3	10.2	0.8	25.8	12.8	18.2	82.5	82.2	53.1	18.0	79.0	31.4	10.4	35.6	41.4	48.2
CAG_UDA [117]	✗	84.8	41.7	85.8	-	-	-	13.7	23.0	86.5	78.1	66.3	28.1	81.8	21.8	22.9	49.0	-	52.6
PLCA [41]		82.6	29.0	81.0	11.2	0.2	33.6	24.9	18.3	82.8	82.3	62.1	26.5	85.6	48.9	26.8	52.2	46.8	54.0
SIM [100]		83.0	44.0	80.3	-	-	-	17.1	15.8	80.5	81.8	59.9	33.1	70.2	37.3	28.5	45.8	-	52.1
FDA [110]		79.3	35.0	73.2	-	-	-	19.9	24.0	61.7	82.6	61.4	31.1	83.9	40.8	38.4	51.1	-	52.5
SFDA [57]		81.9	44.9	81.7	4.0	0.5	26.2	3.3	10.7	86.3	89.4	37.9	13.4	80.6	25.6	9.6	31.3	39.2	45.9
URMA [81]		59.3	24.6	77.0	14.0	1.8	31.5	18.3	32.0	83.1	80.4	46.3	17.8	76.7	17.0	18.5	34.6	39.6	45.0
S4T [78]	✓	84.9	43.2	79.5	7.2	0.3	26.3	7.8	11.7	80.7	82.4	52.4	18.7	77.4	9.6	9.5	37.9	39.3	45.8
SFUDA [111]		90.9	45.5	80.8	3.6	0.5	28.6	8.5	26.1	83.4	83.6	55.2	25.0	79.5	32.8	20.2	43.9	44.2	51.9
HCL [36]		80.9	34.9	76.7	6.6	0.2	36.1	20.1	28.2	79.1	83.1	55.6	25.6	78.8	32.7	24.1	32.7	43.5	50.2
ATP (w/o TP)		89.7	44.6	80.1	3.3	0.3	28.4	8.1	7.7	81.1	85.2	55.2	19.1	83.4	34.3	16.7	32.4	41.8	49.0
ATP (w/o P)	✓	89.8	45.1	82.9	0.1	0.0	33.8	14.6	17.3	84.5	87.0	59.3	25.6	85.8	49.4	26.2	56.1	46.9	55.9
ATP		90.1	46.3	82.5	0.0	0.1	31.7	10.7	17.9	85.1	87.7	64.6	34.6	86.4	54.8	33.7	58.3	49.0	57.9

is empirically set as 10. For the semi-supervised training process, we assign the target images with average entropy ranked top 50% as the easy group, and the other images are defined as the hard group. Generally, we randomly run our methods three times with different random seeds via PyTorch and report the average accuracy.

4.3 Results

In this section, we show the performance of proposed **ATP** on GTA5→Cityscapes in Table 1, SYNTHIA→Cityscapes in Table 2, and Cityscapes→Cross-City in Table 3. **ATP (w/o TP)**, **ATP (w/o P)**, and **ATP** denote results of different training stages, namely implicit feature alignment, bidirectional self-training, and information propagation, respectively. In addition, we compare our method with previous state-of-the-art works, including traditional source data-dependent methods [7], [41], [90], [95], [100], [110], [117], [124] and source data-free methods [36], [57], [78], [81], [111]. The utility of source data can directly align distributions of source and target domains. Thus conventional source data-dependent approaches obtain higher performance than source data-free adaptation methods reasonably. Notice that our method **ATP** performing domain adaptation without source data achieves comparable results or even better than source data-dependent methods. Furthermore, concerning source data-free scenarios, our method outperforms previous works [36], [57], [78], [81], [111] with a large margin.

Specifically, for the tasks of GTA5→Cityscapes and SYNTHIA→Cityscapes, as shown in Table 1 and 2, our method arrives at mIoU scores 52.6% and 57.9%, respectively, which offers a large margin performance gain compared to the non-adaptation baseline. Moreover, the proposed method surpasses four existing source data-free methods SFDA [57], URMA [81], SFUDA [111], and HCL [36], with 9.4%, 7.5%, 3.2%, and 4.5% mIoU scores on GTA5→Cityscapes, and 12.0%, 12.9%, 6.0%, and 7.7% mIoU scores on SYNTHIA→Cityscapes, respectively. Besides, compared with the traditional domain adaptation

approaches that utilize the source data, our method achieves comparable or superior results. These results verify the effectiveness of our method.

In Table 3, we show results on Cityscapes→Cross-City task that has a minor domain shift attribute to both source and target data obtained from real-world datasets. We also compare with conventional source data-dependent domain adaptation approaches [7], [10], [90], [95] and source data-free approaches [57], [81] that provide adaptation results in the original paper. From the results, we can observe that our method **ATP** achieves the best performance in four different adaptation scenarios, including from Cityscapes to Rome, Rio, Tokyo, and Taipei, respectively. It demonstrates the effectiveness of our method for minor domain shift adaptation.

4.4 Extension for Black-box Source Model

In Table 4, we provide the results of the black-box source model case where only the source model’s predictions are available. This situation is more challenging and interesting in practice because it does not require any source model details but the network outputs. Due to no access to trained source model parameters, we use knowledge distill to enforce the target model to learn similarity predictions with the source model, which is considered as the baseline model with 38.6% mIoU performance. After that, we apply the proposed bidirectional self-training strategy and information propagation to tackle the black-box source model scenario. “**ATP (w/o P)**” and “**ATP**” represent our black-box source model on the bidirectional self-training stage and information propagation stage, respectively. Furthermore, we apply data augmentation techniques like “Color Jitter” and “Gaussian Blur” to enhance feature representations. “**ATP (aug)**” denotes the corresponding results. In Table 4, we compare the black-box source model with conventional domain adaptation and source data-free domain adaptation approaches. From the results, we can observe that our method is suitable for the black-box source model situation

TABLE 3: Results of Cityscapes → Cross-City domain adaptation. “SF” denotes the source data-free setting. **Red** is the best result for source data-free methods. **Blue** is the best result for source data-dependent methods.

City	Method	SF	road	side.	build.	light	sign	vege.	sky	person	rider	car	bus	motor.	bike	mIoU
Rome	ADVENT [95]	-	-	-	-	-	-	-	-	-	-	-	-	-	-	47.3
	AdaptSegNet [90]	✗	-	-	-	-	-	-	-	-	-	-	-	-	-	48.0
	Cross-City [10]	79.5	29.3	84.5	0.0	22.2	80.6	82.8	29.5	13.0	71.7	37.5	25.9	1.0	42.9	
	MaxSquare [7]	82.9	32.6	86.7	20.7	41.6	85.0	93.0	47.2	22.5	82.2	53.8	50.5	9.9	54.5	
	SFDA [57]	-	-	-	-	-	-	-	-	-	-	-	-	-	-	48.3
	URMA [81]	86.2	39.1	87.6	14.3	37.8	85.5	88.5	49.9	21.9	81.6	56.3	40.4	10.4	53.8	
	ATP (w/o TP)	✓	80.7	28.6	85.2	13.7	32.6	83.3	85.8	38.9	9.5	78.2	36.9	43.5	9.7	48.2
	ATP (w/o P)		88.4	43.5	89.2	10.4	41.1	87.1	93.4	51.8	4.0	83.7	46.2	45.7	15.5	53.8
	ATP		90.2	46.5	89.7	15.5	40.2	87.4	93.9	54.7	15.5	85.9	48.1	48.6	10.2	55.9
Rio	ADVENT [95]	-	-	-	-	-	-	-	-	-	-	-	-	-	-	46.8
	AdaptSegNet [90]	✗	-	-	-	-	-	-	-	-	-	-	-	-	-	47.8
	Cross-City [10]	74.2	43.9	79.0	2.4	7.5	77.8	69.5	39.3	10.3	67.9	41.2	27.9	10.9	42.5	
	MaxSquare [7]	76.9	48.8	85.2	13.8	18.9	81.7	88.1	54.9	34.0	76.8	39.8	44.1	29.7	53.3	
	SFDA [57]	-	-	-	-	-	-	-	-	-	-	-	-	-	-	49.0
	URMA [81]	82.8	57.0	84.8	17.4	24.0	80.5	86.0	54.2	27.7	78.2	43.8	38.3	21.5	53.5	
	ATP (w/o TP)	✓	73.4	44.1	82.9	9.5	14.0	79.1	81.2	50.5	10.8	71.4	32.3	47.2	36.9	48.7
	ATP (w/o P)		84.7	58.5	86.3	0.8	26.5	82.0	88.1	56.7	23.6	78.1	38.1	50.4	34.4	55.3
	ATP		85.8	60.0	87.8	0.0	29.9	83.6	88.7	60.7	23.3	76.4	43.0	47.4	41.4	57.8
Tokyo	ADVENT [95]	-	-	-	-	-	-	-	-	-	-	-	-	-	-	45.5
	AdaptSegNet [90]	✗	-	-	-	-	-	-	-	-	-	-	-	-	-	46.2
	Cross-City [10]	83.4	35.4	72.8	12.3	12.7	77.4	64.3	42.7	21.5	64.1	20.8	8.9	40.3	42.8	
	MaxSquare [7]	81.2	30.1	77.0	12.3	27.3	82.8	89.5	58.2	32.7	71.5	5.5	37.4	48.9	50.5	
	SFDA [57]	-	-	-	-	-	-	-	-	-	-	-	-	-	-	46.4
	URMA [81]	87.1	38.3	77.2	13.7	24.4	82.6	86.9	54.1	28.0	69.6	18.5	19.2	48.0	49.8	
	ATP (w/o TP)	✓	79.0	25.1	75.0	10.5	21.1	80.3	85.5	48.9	17.2	67.9	5.6	24.8	47.0	45.3
	ATP (w/o P)		88.1	38.2	79.8	0.1	22.6	84.5	89.2	55.5	22.7	72.0	3.7	21.3	52.7	48.6
	ATP		89.9	40.5	83.3	0.0	27.5	85.4	91.7	59.6	22.4	75.4	4.3	14.3	55.1	50.5
Taipei	ADVENT [95]	-	-	-	-	-	-	-	-	-	-	-	-	-	-	45.1
	AdaptSegNet [90]	✗	-	-	-	-	-	-	-	-	-	-	-	-	-	45.1
	Cross-City [10]	78.6	28.6	80.0	13.1	7.6	68.2	82.1	16.8	9.4	60.4	34.0	26.5	9.9	39.6	
	MaxSquare [7]	80.7	32.5	85.5	32.7	15.1	78.1	91.3	32.9	7.6	69.5	44.8	52.4	34.9	50.6	
	SFDA [57]	-	-	-	-	-	-	-	-	-	-	-	-	-	-	47.2
	URMA [81]	86.4	34.6	84.6	22.4	9.9	76.2	88.3	32.8	15.1	74.8	45.8	53.3	26.7	50.1	
	ATP (w/o TP)	✓	73.9	23.3	82.6	20.1	12.2	74.3	86.6	23.2	0.8	63.0	35.2	41.5	31.7	43.6
	ATP (w/o P)		88.1	37.4	86.7	0.0	10.2	79.6	93.2	38.3	3.3	75.9	43.1	55.8	33.3	49.6
	ATP		88.5	39.8	84.6	0.0	11.9	81.0	78.6	43.5	2.6	79.4	51.2	58.7	41.3	51.1

with a performance of 45.3%, achieving comparable results to source data-dependent and source data-free adaptation methods.

4.5 Ablation Study

In this section, we provide extensive experiments to verify the effectiveness of the proposed **ATP**. Specifically, we first reveal the improvement of proposed components on GTA5 → Cityscapes task by progressively adding each module into the system. As Table 5 shows, we can observe that each component contributes to adaptation, with achieving the final performance of 52.6% mIoU on the source data-free scenario. Then, we conduct experiments on different segmentation backbones to verify the generalization of our method. The details are described as follows.

Influence of implicit feature alignment. From the models (a) and (b) in Table 5, we can observe that our curriculum-style entropy loss (\mathcal{L}_{cel}) and weighted diversity loss (\mathcal{L}_{div}) can significantly improve adaptation performance. Specifically, model (a) with \mathcal{L}_{cel} achieves a 43.6% mIoU result, which surpasses the baseline model by 4.3 points. It also significantly outperforms the previous entropy minimization method [81] reported mIoU result as

19.8%. Furthermore, model (b) with \mathcal{L}_{div} boosts the performance improvement with 1.4 mIoU, revealing that diversity enforcing is important for our setting. \mathcal{L}_{div}^* denotes diversity loss provided by [53] with the mean output embedding. Compared model (b) with (c), we see that both diversity-promoting terms are beneficial for our task, and the proposed weighted one (\mathcal{L}_{div}) works better than a non-weighted one (\mathcal{L}_{div}^*).

Influence of bidirectional self-training. To verify the effectiveness of the proposed bidirectional self-training method, we ablate the positive pseudo labeling \mathcal{L}_{ppl} and negative pseudo labeling \mathcal{L}_{npl} , respectively. The results show that model (d) trained from the only positive pseudo labeling provides 2.7 point gains compared to model (b). It is reasonable that the positive pseudo labels provide useful supervised information for the target data. On the other hand, adding the negative pseudo labeling (model (e)) fancily offers 2.1 point improvement further. This result demonstrates that negative pseudo labels can provide complementary information which is ignored by the traditional positive pseudo labeling methods. Both the positive and negative pseudo labeling are helpful to learn decision boundaries.

Influence of information propagation. To testify the

TABLE 4: Results of *black-box* source model on GTA5 → Cityscapes domain adaptation. “SF” denotes the source data-free setting. Gray row group denotes results of our black-box source model.

Method	SF	road	side.	build.	wall	fence	pole	light	sign	vege.	terr.	sky	person	rider	car	truck	bus	train	motor.	bike	mIoU
AdaptSegNet [40]		86.5	36.0	79.9	23.4	23.3	23.9	35.2	14.8	83.4	33.3	75.6	58.5	27.6	73.7	32.5	35.4	3.9	30.1	28.1	42.4
ADVENT [43]		89.4	33.1	81.0	26.6	26.8	27.2	33.5	24.7	83.9	36.7	78.8	58.7	30.5	84.8	38.5	44.5	1.7	31.6	32.4	45.5
CBST [57]	✗	91.8	53.5	80.5	32.7	21.0	34.0	28.9	20.4	83.9	34.2	80.9	53.1	24.0	82.7	30.3	35.9	16.0	25.9	42.8	45.9
MaxSquare [4]		89.4	43.0	82.1	30.5	21.3	30.3	34.7	24.0	85.3	39.4	78.2	63.0	22.9	84.6	36.4	43.0	5.5	34.7	33.5	46.4
PLCA [15]		84.0	30.4	82.4	35.3	24.8	32.2	36.8	24.5	85.5	37.2	78.6	66.9	32.8	85.5	40.4	48.0	8.8	29.8	41.8	47.7
SFDA [25]		84.2	39.2	82.7	27.5	22.1	25.9	31.1	21.9	82.4	30.5	85.3	58.7	22.1	80.0	33.1	31.5	3.6	27.8	30.6	43.2
URMA [35]	✓	92.3	55.2	81.6	30.8	18.8	37.1	17.7	12.1	84.2	35.9	83.8	57.7	24.1	81.7	27.5	44.3	6.9	24.1	40.4	45.1
S4T [78]		89.7	39.2	84.4	25.7	29.0	39.5	45.1	36.8	86.8	41.8	79.3	61.2	26.7	85.0	19.3	28.2	5.3	11.8	9.3	44.8
Baseline	-	75.5	25.4	80.8	20.2	25.0	10.9	17.5	0.0	84.4	16.0	83.5	58.7	0.0	80.5	34.9	46.1	0.0	31.9	42.0	38.6
ATP (w/o P)		74.8	23.6	78.9	27.4	17.5	24.1	34.0	24.9	82.6	25.7	74.3	58.6	31.7	71.5	31.4	6.9	0.0	34.8	45.4	40.4
ATP	✓	83.3	24.2	80.3	29.7	22.4	26.3	33.0	25.5	84.7	35.7	76.6	61.9	34.0	81.7	32.1	17.3	0.0	42.1	53.4	44.4
ATP (aug)		83.6	25.8	81.9	30.2	25.2	27.9	36.2	28.7	84.8	34.4	77.5	62.2	35.7	81.5	32.3	16.8	0.0	41.7	53.5	45.3

TABLE 5: Ablation study of each component on GTA5 → Cityscapes domain adaptation task.

Model	\mathcal{L}_{cel}	\mathcal{L}_{div}	\mathcal{L}_{div}^*	\mathcal{L}_{ppl}	\mathcal{L}_{npl}	\mathcal{L}_{ssl}	mIoU
Baseline							39.3
(a)	✓						43.6
(b)	✓	✓					45.0
(c)	✓		✓				43.9
(d)	✓	✓		✓			47.7
(e)	✓	✓		✓	✓		49.8
(f)	✓	✓		✓	✓	✓	52.6

TABLE 6: Results on different SSL approaches on GTA5 → Cityscapes task.

ratio	Baseline	CutMix [113]	ClassMix [70]	ReCo [56]
0.5	49.8	50.4	52.6	51.9
0.3	49.8	50.6	52.1	51.4

effectiveness of the information propagation strategy, we follow several semi-supervised learning methods in our approach, including consistency learning technique (CutMix [113], ClassMix [70]) and contrastive learning technique (ReCo [56]). We report the best result obtained from ClassMix model (f) in Table 5, which provides a significant improvement with 2.8 mIoU compared to model (e). It demonstrates that the semi-supervised technique is simple and effective for reducing intra-domain discrepancy. Detailed results of the information propagation stage are shown in Table 6. In this subsection, two consistency learning based methods (CutMix [113], ClassMix [70]) and one contrastive learning based method (ReCo [56]) are adopted. The parameter *ratio* denotes the proportion of easy split on the whole target dataset.

Performance on different backbones. To demonstrate the robustness of our method, we apply different backbones to conduct the semantic segmentation network. In

TABLE 7: Domain adaptation results of GTA5 → Cityscapes task based on VGG-16 network.

Method	SF	mIoU
Baseline	-	27.1
ADVENT [95]	✗	35.6
AdaptSegNet [90]	✗	35.0
CLAN [63]	✗	36.6
CyCADA [32]	✗	35.4
PatchDA [91]	✗	37.5
SSF-DAN [17]	✗	37.7
ATP (Ours)	✓	39.8

this section, we utilize VGG-16 [85] networks as a segmentation feature extractor, and the final adaptation performance is shown in Table 7. We compare existing source data-dependent domain adaptation works that report results based on VGG-16 networks. We can observe that our method surpasses existing conventional source data-dependent domain adaptation approaches with achieving 39.8% mIoU, which reveals the proposed ATP is robust for different backbone networks.

4.6 Parameter Sensitivity Analysis

Our framework contains two new hyper-parameters α and γ in Eq. (2). To analyze the influence, we conduct experiments on the GTA5 → Cityscapes task. We first freeze γ and choose $\alpha = 0.002$ from the range of [0.001, 0.002, 0.003], and then the value of γ is selected as 3 from the range of [0, 1, 2, 3, 4, 5]. The results are shown in Figure 5. Although all experiments set $\alpha = 0.002$ and $\gamma = 3$ since it peaks, we observe that the proposed curriculum-style entropy loss is relatively robust to these parameters. Besides, we also optimize the model without freezing the source classifier. The performance drops significantly compared to those with frozen classifier, which indicates that the hypothesis transfer with frozen classifier is essential.

Figure 6 shows results when varying the assignment threshold λ_{neg} related to negative pseudo labels in Eq. (6). It

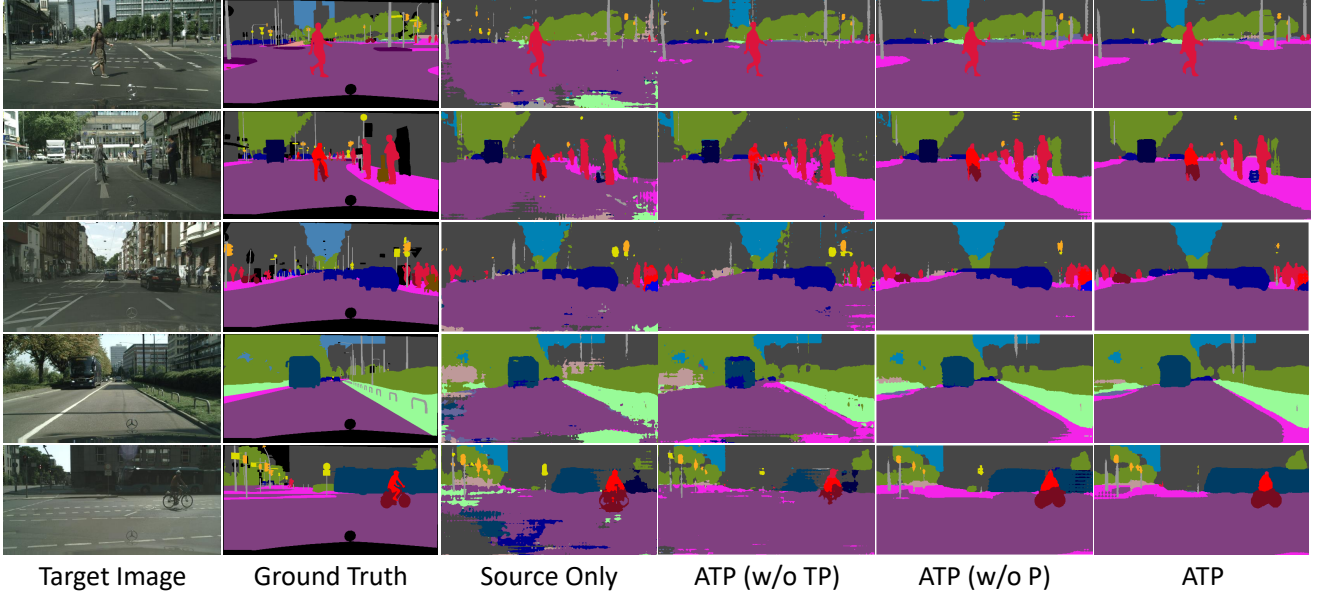


Fig. 4: Visualization for predicted segmentation masks on the GTA5→Cityscapes task.

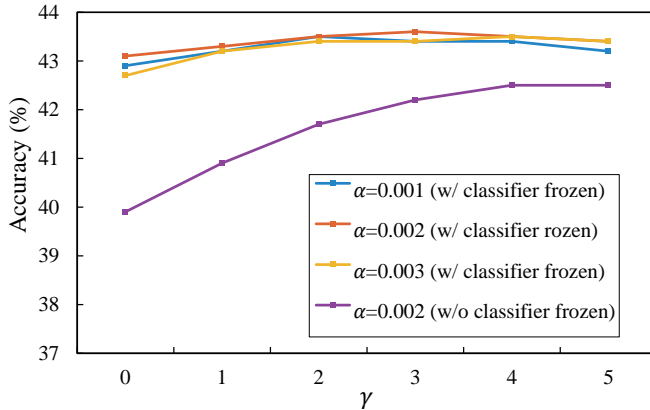
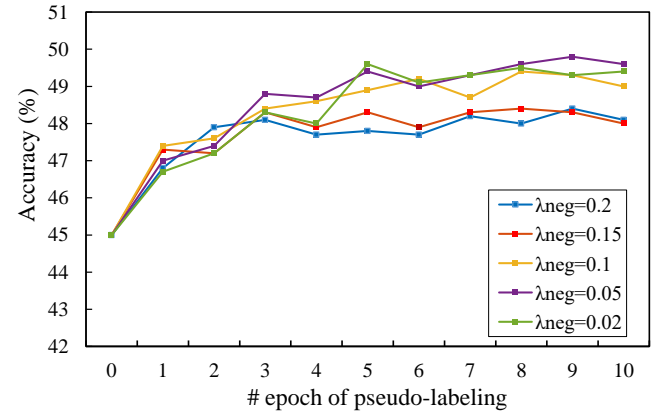
Fig. 5: Analysis for the hyper-parameters α and γ of the proposed adaptive entropy loss.

TABLE 8: Results of different pseudo-labeling thresholds in Eq. (4) on GTA5→Cityscapes task.

Top- K	0.85	0.80	0.75	0.70	0.65	0.60
mIoU	47.5	47.4	47.0	47.3	47.7	47.1

shows that the proposed negative pseudo labeling method is relatively robust to this hyper-parameter. Moreover, the proposed method quickly converges after several training epochs. We also observe that $\lambda_{neg} < 0.1$ obtains a satisfactory performance compared to those when $\lambda_{neg} > 0.1$. The reason is that more noise labels are introduced when the threshold increases as our negative pseudo labeling method focuses on predictions with lower confidence scores.

More hyper-parameters introduced in this paper are analyzed in this subsection. We provide the risk of target supervision leak in the bidirectional self-training stage. For example, in Table 8, we report the influence of the pseudo-labeling threshold λ_c in Eq. (4), which is determined by the

Fig. 6: Robustness to the negative threshold λ_{neg} for the negative pseudo assignment method.TABLE 9: Results of different weights λ for weighted diversity loss in Eq. (3) on GTA5→Cityscapes task.

λ	1	2	3	4	5
mIoU	44.0	44.2	45.0	44.1	44.0

top- K . In Table 9, we also analyze the weight λ for weighted diversity loss in Eq. (3), which controls the influence of weighted mean output $\hat{p}_{x_t}^{(h,w,c)}$.

4.7 Visualization

In Figure 4, we visualize predicted segmentation masks obtained from our method and compare the results to the masks predicted by the “Source-Only” network. To show the contribution of each stage, we add each component progressively and provide qualitative results of “ATP (w/o TP)”, “ATP (w/o P)”, and “ATP”, respectively. It is evident that even without source data, our method achieves reliable results with fewer spurious areas. Furthermore, compared

to the “Source Only” model, each stage contributes significantly in terms of pixel-level accuracy.

5 CONCLUSION

This paper presents a novel source data-free framework for domain adaptive semantic segmentation called **ATP**. In the absence of source data, **ATP** focuses on transferring knowledge from the source model via implicit feature alignment, teaching from positive and negative pseudo labels, and propagating target-specific information to reduce the intra-domain discrepancy. Extensive experiments and ablation studies are conducted to validate the effectiveness of the proposed **ATP**. On the standard adaptation tasks, **ATP** achieves new state-of-the-art results and performs comparably to source data-dependent adaptation methods. It also performs well on the black-box source model scenario.

In the future, we will attempt to tackle two critical problems. The first is to improve the performance of hard categories. As Table 1 and Table 2 show, the proposed method fails to handle some classes with a large domain gap or occupy a minor pixel proportion, like fence, pole, signal, and train. It is a common but serious problem to address for DASS. The second is the selection of hyper-parameters. In our work, we introduce amounts of hyper-parameters that influence the final performance. It is essential to provide a method to learn overall generality and robust hyperparameter in future work.

ACKNOWLEDGEMENT

This work is jointly supported by the Major Project for New Generation of AI (No.2018AAA0100400), and the National Natural Science Foundation of China (No. 61836014, No. U21B2042, No. 62072457, No. 62006231).

REFERENCES

- [1] S. M. Ahmed, D. S. Raychaudhuri, S. Paul, S. Oymak, and A. K. Roy-Chowdhury. Unsupervised multi-source domain adaptation without access to source data. In *Proc. CVPR*, pages 10103–10112, 2021.
- [2] D. Berthelot, N. Carlini, E. D. Cubuk, A. Kurakin, K. Sohn, H. Zhang, and C. Raffel. Remixmatch: Semi-supervised learning with distribution alignment and augmentation anchoring. In *Proc. ICLR*, 2019.
- [3] K. Bousmalis, G. Trigeorgis, N. Silberman, D. Krishnan, and D. Erhan. Domain separation networks. In *Proc. NeurIPS*, volume 29, 2016.
- [4] L. Bruzzone and M. Marconcini. Domain adaptation problems: A dasvm classification technique and a circular validation strategy. *IEEE Transactions on Pattern Analysis and Machine Intelligence*, 32(5):770–787, 2009.
- [5] W.-L. Chang, H.-P. Wang, W.-H. Peng, and W.-C. Chiu. All about structure: Adapting structural information across domains for boosting semantic segmentation. In *Proc. CVPR*, pages 1900–1909, 2019.
- [6] L.-C. Chen, G. Papandreou, I. Kokkinos, K. Murphy, and A. L. Yuille. Deeplab: Semantic image segmentation with deep convolutional nets, atrous convolution, and fully connected crfs. *IEEE Transactions on Pattern Analysis and Machine Intelligence*, 40(4):834–848, 2017.
- [7] M. Chen, H. Xue, and D. Cai. Domain adaptation for semantic segmentation with maximum squares loss. In *Proc. ICCV*, pages 2090–2099, 2019.
- [8] Y. Chen, W. Li, C. Sakaridis, D. Dai, and L. Van Gool. Domain adaptive faster r-cnn for object detection in the wild. In *Proc. CVPR*, pages 3339–3348, 2018.
- [9] Y.-C. Chen, Y.-Y. Lin, M.-H. Yang, and J.-B. Huang. Crdoco: Pixel-level domain transfer with cross-domain consistency. In *Proc. CVPR*, pages 1791–1800, 2019.
- [10] Y.-H. Chen, W.-Y. Chen, Y.-T. Chen, B.-C. Tsai, Y.-C. Frank Wang, and M. Sun. No more discrimination: Cross city adaptation of road scene segmenters. In *Proc. ICCV*, pages 1992–2001, 2017.
- [11] Y. Cheng, F. Wei, J. Bao, D. Chen, F. Wen, and W. Zhang. Dual path learning for domain adaptation of semantic segmentation. In *Proc. ICCV*, pages 9082–9091, 2021.
- [12] B. Chidlovskii, S. Clinchant, and G. Csurka. Domain adaptation in the absence of source domain data. In *Proc. KDD*, pages 451–460, 2016.
- [13] J. Choi, T. Kim, and C. Kim. Self-ensembling with gan-based data augmentation for domain adaptation in semantic segmentation. In *Proc. ICCV*, pages 6830–6840, 2019.
- [14] S. Cicek and S. Soatto. Unsupervised domain adaptation via regularized conditional alignment. In *Proc. ICCV*, pages 1416–1425, 2019.
- [15] M. Cordts, M. Omran, S. Ramos, T. Rehfeld, M. Enzweiler, R. Benenson, U. Franke, S. Roth, and B. Schiele. The cityscapes dataset for semantic urban scene understanding. In *Proc. CVPR*, pages 3213–3223, 2016.
- [16] J. Deng, W. Dong, R. Socher, L.-J. Li, K. Li, and L. Fei-Fei. Imagenet: A large-scale hierarchical image database. In *Proc. CVPR*, pages 248–255, 2009.
- [17] L. Du, J. Tan, H. Yang, J. Feng, X. Xue, Q. Zheng, X. Ye, and X. Zhang. Ssf-dan: Separated semantic feature based domain adaptation network for semantic segmentation. In *Proc. ICCV*, pages 982–991, 2019.
- [18] Y. Fan, R. He, J. Liang, and B. Hu. Self-paced learning: An implicit regularization perspective. In *Proc. AAAI*, volume 31, 2017.
- [19] H. Feng, M. Chen, J. Hu, D. Shen, H. Liu, and D. Cai. Complementary pseudo labels for unsupervised domain adaptation on person re-identification. *IEEE Transactions on Image Processing*, 30:2898–2907, 2021.
- [20] R. Flamary, N. Courty, D. Tuia, and A. Rakotomamonjy. Optimal transport for domain adaptation. *IEEE Transactions on Pattern Analysis and Machine Intelligence*, 39(9):1853–1865, 2017.
- [21] Y. Fu, Y. Wei, G. Wang, Y. Zhou, H. Shi, and T. S. Huang. Self-similarity grouping: A simple unsupervised cross domain adaptation approach for person re-identification. In *Proc. ICCV*, pages 6112–6121, 2019.
- [22] Y. Ganin and V. Lempitsky. Unsupervised domain adaptation by backpropagation. In *Proc. ICML*, pages 1180–1189, 2015.
- [23] Y. Ge, F. Zhu, D. Chen, R. Zhao, et al. Self-paced contrastive learning with hybrid memory for domain adaptive object re-id. In *Proc. NeurIPS*, volume 33, pages 11309–11321, 2020.
- [24] M. Ghifary, W. B. Kleijn, M. Zhang, D. Balduzzi, and W. Li. Deep reconstruction-classification networks for unsupervised domain adaptation. In *Proc. ECCV*, pages 597–613, 2016.
- [25] B. Gong, K. Grauman, and F. Sha. Connecting the dots with landmarks: Discriminatively learning domain-invariant features for unsupervised domain adaptation. In *Proc. ICML*, pages 222–230, 2013.
- [26] I. Goodfellow, J. Pouget-Abadie, M. Mirza, B. Xu, D. Warde-Farley, S. Ozair, A. Courville, and Y. Bengio. Generative adversarial nets. In *Proc. NeurIPS*, volume 27, 2014.
- [27] R. Gopalan, R. Li, V. M. Patel, and R. Chellappa. Domain adaptation for visual recognition. *Foundations and Trends® in Computer Graphics and Vision*, 8(4):285–378, 2015.
- [28] D. Guan, J. Huang, A. Xiao, S. Lu, and Y. Cao. Uncertainty-aware unsupervised domain adaptation in object detection. *IEEE Transactions on Multimedia*, 2021.
- [29] J. Guo, X. Zhu, Z. Lei, and S. Z. Li. Decomposed meta batch normalization for fast domain adaptation in face recognition. *IEEE Transactions on Information Forensics and Security*, 16:3082–3095, 2021.
- [30] K. He, X. Zhang, S. Ren, and J. Sun. Deep residual learning for image recognition. In *Proc. CVPR*, pages 770–778, 2016.
- [31] G. Hinton, O. Vinyals, J. Dean, et al. Distilling the knowledge in a neural network. *arXiv preprint arXiv:1503.02531*, 2(7), 2015.
- [32] J. Hoffman, E. Tzeng, T. Park, J.-Y. Zhu, P. Isola, K. Saenko, A. Efros, and T. Darrell. CyCADA: Cycle-consistent adversarial domain adaptation. In *Proc. ICML*, pages 1989–1998, 2018.
- [33] J. Hoffman, D. Wang, F. Yu, and T. Darrell. Fcn in the wild: Pixel-level adversarial and constraint-based adaptation. *arXiv preprint arXiv:1612.02649*, 2016.
- [34] W. Hong, Z. Wang, M. Yang, and J. Yuan. Conditional generative adversarial network for structured domain adaptation. In *Proc. CVPR*, pages 1335–1344, 2018.

[35] H. Huang, Q. Huang, and P. Krahnenbuhl. Domain transfer through deep activation matching. In *Proc. ECCV*, pages 590–605, 2018.

[36] J. Huang, D. Guan, A. Xiao, and S. Lu. Model adaptation: Historical contrastive learning for unsupervised domain adaptation without source data. In *Proc. NeurIPS*, volume 34, 2021.

[37] J. Huang, S. Lu, D. Guan, and X. Zhang. Contextual-relation consistent domain adaptation for semantic segmentation. In *Proc. ECCV*, pages 705–722, 2020.

[38] W. C. Hung, Y. H. Tsai, Y. T. Liou, Y. Y. Lin, and M. H. Yang. Adversarial learning for semi-supervised semantic segmentation. In *Proc. BMVC*, 2019.

[39] M. Kan, J. Wu, S. Shan, and X. Chen. Domain adaptation for face recognition: Targetize source domain bridged by common subspace. *International Journal of Computer Vision*, 109(1):94–109, 2014.

[40] G. Kang, L. Jiang, Y. Yang, and A. G. Hauptmann. Contrastive adaptation network for unsupervised domain adaptation. In *Proc. CVPR*, pages 4893–4902, 2019.

[41] G. Kang, Y. Wei, Y. Yang, Y. Zhuang, and A. Hauptmann. Pixel-level cycle association: A new perspective for domain adaptive semantic segmentation. In *Proc. NeurIPS*, pages 3569–3580, 2020.

[42] M. Kim and H. Byun. Learning texture invariant representation for domain adaptation of semantic segmentation. In *Proc. CVPR*, pages 12975–12984, 2020.

[43] M. Kumar, B. Packer, and D. Koller. Self-paced learning for latent variable models. In *Proc. NeurIPS*, pages 1189–1197, 2010.

[44] J. N. Kundu, A. Kulkarni, A. Singh, V. Jampani, and R. V. Babu. Generalize then adapt: Source-free domain adaptive semantic segmentation. In *Proc. ICCV*, pages 7046–7056, 2021.

[45] J. N. Kundu, N. Venkat, R. V. Babu, et al. Universal source-free domain adaptation. In *Proc. CVPR*, pages 4544–4553, 2020.

[46] V. K. Kurmi and V. P. Namboodiri. Looking back at labels: A class based domain adaptation technique. In *Proc. IJCNN*, pages 1–8. IEEE, 2019.

[47] S. Lee, D. Kim, N. Kim, and S.-G. Jeong. Drop to adapt: Learning discriminative features for unsupervised domain adaptation. In *Proc. ICCV*, pages 91–100, 2019.

[48] R. Li, Q. Jiao, W. Cao, H.-S. Wong, and S. Wu. Model adaptation: Unsupervised domain adaptation without source data. In *Proc. CVPR*, pages 9641–9650, 2020.

[49] Y. Li, L. Yuan, and N. Vasconcelos. Bidirectional learning for domain adaptation of semantic segmentation. In *Proc. CVPR*, pages 6936–6945, 2019.

[50] Q. Lian, F. Lv, L. Duan, and B. Gong. Constructing self-motivated pyramid curriculums for cross-domain semantic segmentation: A non-adversarial approach. In *Proc. ICCV*, pages 6758–6767, 2019.

[51] J. Liang, R. He, Z. Sun, and T. Tan. Aggregating randomized clustering-promoting invariant projections for domain adaptation. *IEEE Transactions on Pattern Analysis and Machine Intelligence*, 41(5):1027–1042, 2018.

[52] J. Liang, R. He, Z. Sun, and T. Tan. Distant supervised centroid shift: A simple and efficient approach to visual domain adaptation. In *Proc. CVPR*, pages 2975–2984, 2019.

[53] J. Liang, D. Hu, and J. Feng. Do we really need to access the source data? source hypothesis transfer for unsupervised domain adaptation. In *Proc. ICML*, pages 6028–6039, 2020.

[54] J. Liang, D. Hu, J. Feng, and R. He. Dine: Domain adaptation from single and multiple black-box predictors. In *Proc. CVPR*, 2022.

[55] T.-Y. Lin, P. Goyal, R. Girshick, K. He, and P. Dollár. Focal loss for dense object detection. In *Proc. ICCV*, pages 2980–2988, 2017.

[56] S. Liu, S. Zhi, E. Johns, and A. J. Davison. Bootstrapping semantic segmentation with regional contrast. *arXiv preprint arXiv:2104.04465*, 2021.

[57] Y. Liu, W. Zhang, and J. Wang. Source-free domain adaptation for semantic segmentation. In *Proc. CVPR*, pages 1215–1224, 2021.

[58] J. Long, E. Shelhamer, and T. Darrell. Fully convolutional networks for semantic segmentation. In *Proc. CVPR*, pages 3431–3440, 2015.

[59] M. Long, Y. Cao, Z. Cao, J. Wang, and M. I. Jordan. Transferable representation learning with deep adaptation networks. *IEEE Transactions on Pattern Analysis and Machine Intelligence*, 41(12):3071–3085, 2018.

[60] M. Long, Y. Cao, J. Wang, and M. Jordan. Learning transferable features with deep adaptation networks. In *Proc. ICML*, pages 97–105, 2015.

[61] M. Long, Z. Cao, J. Wang, and M. I. Jordan. Conditional adversarial domain adaptation. In *Proc. NeurIPS*, volume 31, 2018.

[62] W. Luo and M. Yang. Semi-supervised semantic segmentation via strong-weak dual-branch network. In *Proc. ECCV*, pages 784–800, 2020.

[63] Y. Luo, L. Zheng, T. Guan, J. Yu, and Y. Yang. Taking a closer look at domain shift: Category-level adversaries for semantics consistent domain adaptation. In *Proc. CVPR*, pages 2507–2516, 2019.

[64] F. Maria Carlucci, L. Porzi, B. Caputo, E. Ricci, and S. Rota Bulo. Autodial: Automatic domain alignment layers. In *Proc. ICCV*, pages 5067–5075, 2017.

[65] K. Mei, C. Zhu, J. Zou, and S. Zhang. Instance adaptive self-training for unsupervised domain adaptation. In *Proc. ECCV*, pages 415–430, 2020.

[66] D. Mekhazni, A. Bhuiyan, G. Ekladious, and E. Granger. Unsupervised domain adaptation in the dissimilarity space for person re-identification. In *Proc. ECCV*, pages 159–174, 2020.

[67] S. Mittal, M. Tatarchenko, and T. Brox. Semi-supervised semantic segmentation with high- and low-level consistency. *IEEE Transactions on Pattern Analysis and Machine Intelligence*, 43(4):1369–1379, 2019.

[68] T. Miyato, S.-i. Maeda, M. Koyama, and S. Ishii. Virtual adversarial training: a regularization method for supervised and semi-supervised learning. *IEEE Transactions on Pattern Analysis and Machine Intelligence*, 41(8):1979–1993, 2018.

[69] Z. Murez, S. Kolouri, D. Kriegman, R. Ramamoorthi, and K. Kim. Image to image translation for domain adaptation. In *Proc. CVPR*, pages 4500–4509, 2018.

[70] V. Olsson, W. Tranleden, J. Pinto, and L. Svensson. Classmix: Segmentation-based data augmentation for semi-supervised learning. In *Proc. WACV*, pages 1369–1378, 2021.

[71] Y. Ouali, C. Hudelot, and M. Tami. Semi-supervised semantic segmentation with cross-consistency training. In *Proc. CVPR*, pages 12674–12684, 2020.

[72] F. Pan, I. Shin, F. Rameau, S. Lee, and I. S. Kweon. Unsupervised intra-domain adaptation for semantic segmentation through self-supervision. In *Proc. ICCV*, pages 3764–3773, 2020.

[73] S. J. Pan, I. W. Tsang, J. T. Kwok, and Q. Yang. Domain adaptation via transfer component analysis. *IEEE Transactions on Neural Networks*, 22(2):199–210, 2010.

[74] S. J. Pan and Q. Yang. A survey on transfer learning. *IEEE Transactions on Knowledge and Data Engineering*, 22(10):1345–1359, 2009.

[75] S. Paul, Y.-H. Tsai, S. Schulter, A. K. Roy-Chowdhury, and M. Chandraker. Domain adaptive semantic segmentation using weak labels. In *Proc. ECCV*, pages 571–587. Springer, 2020.

[76] Z. Pei, Z. Cao, M. Long, and J. Wang. Multi-adversarial domain adaptation. In *Proc. AAAI*, pages 3934–3941, 2018.

[77] J. Peng, P. Wang, C. Desrosiers, and M. Pedersoli. Self-paced contrastive learning for semi-supervised medical image segmentation with meta-labels. In *Proc. NeurIPS*, volume 34, 2021.

[78] V. Prabhu, S. Khare, D. Kartik, and J. Hoffman. S4t: Source-free domain adaptation for semantic segmentation via self-supervised selective self-training. *arXiv preprint arXiv:2107.10140*, 2021.

[79] S. R. Richter, V. Vineet, S. Roth, and V. Koltun. Playing for data: Ground truth from computer games. In *Proc. ECCV*, pages 102–118, 2016.

[80] G. Ros, L. Sellart, J. Materzynska, D. Vazquez, and A. M. Lopez. The synthia dataset: A large collection of synthetic images for semantic segmentation of urban scenes. In *Proc. CVPR*, pages 3234–3243, 2016.

[81] P. T. S and F. Fleuret. Uncertainty reduction for model adaptation in semantic segmentation. In *Proc. CVPR*, pages 9613–9623, 2021.

[82] K. Saito, D. Kim, P. Teterwak, S. Sclaroff, T. Darrell, and K. Saenko. Tune it the right way: Unsupervised validation of domain adaptation via soft neighborhood density. In *Proc. ICCV*, pages 9184–9193, 2021.

[83] K. Saito, Y. Ushiku, T. Harada, and K. Saenko. Adversarial dropout regularization. In *Proc. ICLR*, 2018.

[84] C. Sakaridis, D. Dai, and L. Van Gool. Map-guided curriculum domain adaptation and uncertainty-aware evaluation for semantic nighttime image segmentation. *IEEE Transactions on Pattern Analysis and Machine Intelligence*, (01):1–1, 2020.

[85] K. Simonyan and A. Zisserman. Very deep convolutional networks for large-scale image recognition. In *Proc. ICLR*, 2015.

[86] N. Souly, C. Spampinato, and M. Shah. Semi-supervised semantic segmentation using generative adversarial network. In *Proc. ICCV*, pages 5688–5696, 2017.

[87] M. N. Subhani and M. Ali. Learning from scale-invariant examples for domain adaptation in semantic segmentation. In *Proc. ECCV*, pages 290–306, 2020.

[88] M. Sugiyama, S. Nakajima, H. Kashima, P. Buenau, and

M. Kawanabe. Direct importance estimation with model selection and its application to covariate shift adaptation. In *Proc. NeurIPS*, volume 20, 2007.

[89] T.-D. Truong, C. N. Duong, N. Le, S. L. Phung, C. Rainwater, and K. Luu. Bimal: Bijective maximum likelihood approach to domain adaptation in semantic scene segmentation. In *Proc. ICCV*, pages 8548–8557, 2021.

[90] Y.-H. Tsai, W.-C. Hung, S. Schulter, K. Sohn, M.-H. Yang, and M. Chandraker. Learning to adapt structured output space for semantic segmentation. In *Proc. CVPR*, pages 7472–7481, 2018.

[91] Y.-H. Tsai, K. Sohn, S. Schulter, and M. Chandraker. Domain adaptation for structured output via discriminative patch representations. In *Proc. ICCV*, pages 1456–1465, 2019.

[92] E. Tzeng, J. Hoffman, K. Saenko, and T. Darrell. Adversarial discriminative domain adaptation. In *Proc. CVPR*, pages 7167–7176, 2017.

[93] V. Verma, A. Lamb, J. Kannala, Y. Bengio, and D. Lopez-Paz. Interpolation consistency training for semi-supervised learning. In *Proc. IJCAI*, pages 3635–3641, 2019.

[94] V. VS, V. Gupta, P. Oza, V. A. Sindagi, and V. M. Patel. Megacda: Memory guided attention for category-aware unsupervised domain adaptive object detection. In *Proc. CVPR*, pages 4516–4526, 2021.

[95] T.-H. Vu, H. Jain, M. Bucher, M. Cord, and P. Pérez. Advent: Adversarial entropy minimization for domain adaptation in semantic segmentation. In *Proc. CVPR*, pages 2517–2526, 2019.

[96] M. Wang and W. Deng. Deep visual domain adaptation: A survey. *Neurocomputing*, 312:135–153, 2018.

[97] X. Wang, Y. Chen, and W. Zhu. A survey on curriculum learning. *IEEE Transactions on Pattern Analysis and Machine Intelligence*, (01):1–1, 2021.

[98] X. Wang, L. Li, W. Ye, M. Long, and J. Wang. Transferable attention for domain adaptation. In *Proc. AAAI*, volume 33, pages 5345–5352, 2019.

[99] Y. Wang, J. Peng, and Z. Zhang. Uncertainty-aware pseudo label refinery for domain adaptive semantic segmentation. In *Proc. ICCV*, pages 9092–9101, 2021.

[100] Z. Wang, M. Yu, Y. Wei, R. Feris, J. Xiong, W.-m. Hwu, T. S. Huang, and H. Shi. Differential treatment for stuff and things: A simple unsupervised domain adaptation method for semantic segmentation. In *Proc. CVPR*, pages 12635–12644, 2020.

[101] Z. Wu, X. Han, Y.-L. Lin, M. Gokhan Uzunbas, T. Goldstein, S. Nam Lim, and L. S. Davis. Dcan: Dual channel-wise alignment networks for unsupervised scene adaptation. In *Proc. ECCV*, pages 518–534, 2018.

[102] H. Xia, H. Zhao, and Z. Ding. Adaptive adversarial network for source-free domain adaptation. In *Proc. ICCV*, pages 9010–9019, 2021.

[103] Q. Xie, Z. Dai, E. Hovy, T. Luong, and Q. Le. Unsupervised data augmentation for consistency training. In *Proc. NeurIPS*, pages 6256–6268, 2020.

[104] H. Yan, Y. Guo, and C. Yang. Augmented self-labeling for source-free unsupervised domain adaptation. In *NeurIPS 2021 Workshop on Distribution Shifts: Connecting Methods and Applications*, 2021.

[105] F. Yang, K. Yan, S. Lu, H. Jia, D. Xie, Z. Yu, X. Guo, F. Huang, and W. Gao. Part-aware progressive unsupervised domain adaptation for person re-identification. *IEEE Transactions on Multimedia*, 23:1681–1695, 2020.

[106] J. Yang, W. An, S. Wang, X. Zhu, C. Yan, and J. Huang. Label-driven reconstruction for domain adaptation in semantic segmentation. In *Proc. ECCV*, pages 480–498, 2020.

[107] J. Yang, C. Li, W. An, H. Ma, Y. Guo, Y. Rong, P. Zhao, and J. Huang. Exploring robustness of unsupervised domain adaptation in semantic segmentation. In *Proc. ICCV*, pages 9194–9203, 2021.

[108] J. Yang, S. Shi, Z. Wang, H. Li, and X. Qi. St3d: Self-training for unsupervised domain adaptation on 3d object detection. In *Proc. CVPR*, pages 10368–10378, 2021.

[109] S. Yang, Y. Wang, J. van de Weijer, L. Herranz, and S. Jui. Generalized source-free domain adaptation. In *Proc. ICCV*, pages 8978–8987, 2021.

[110] Y. Yang and S. Soatto. Fda: Fourier domain adaptation for semantic segmentation. In *Proc. CVPR*, pages 4085–4095, 2020.

[111] M. Ye, J. Zhang, J. Ouyang, and D. Yuan. Source data-free unsupervised domain adaptation for semantic segmentation. In *Proc. ACM MM*, pages 2233–2242, 2021.

[112] J. Yuan, Y. Liu, C. Shen, Z. Wang, and H. Li. A simple baseline for semi-supervised semantic segmentation with strong data augmentation. In *Proc. ICCV*, pages 8229–8238, 2021.

[113] S. Yun, D. Han, S. J. Oh, S. Chun, J. Choe, and Y. Yoo. Cutmix: Regularization strategy to train strong classifiers with localizable features. In *Proc. ICCV*, pages 6023–6032, 2019.

[114] B. Zadrozny. Learning and evaluating classifiers under sample selection bias. In *Proc. ICML*, page 114, 2004.

[115] W. Zellinger, T. Grubinger, E. Lughofer, T. Natschläger, and S. Saminger-Platz. Central moment discrepancy (cmd) for domain-invariant representation learning. In *Proc. ICLR*, 2017.

[116] P. Zhang, B. Zhang, T. Zhang, D. Chen, Y. Wang, and F. Wen. Prototypical pseudo label denoising and target structure learning for domain adaptive semantic segmentation. In *Proc. CVPR*, pages 12414–12424, 2021.

[117] Q. Zhang, J. Zhang, W. Liu, and D. Tao. Category anchor-guided unsupervised domain adaptation for semantic segmentation. In *Proc. NeurIPS*, pages 433–443, 2019.

[118] Y. Zhang, P. David, and B. Gong. Curriculum domain adaptation for semantic segmentation of urban scenes. In *Proc. ICCV*, pages 2020–2030, 2017.

[119] Y. Zhang, T. Liu, M. Long, and M. Jordan. Bridging theory and algorithm for domain adaptation. In *Proc. ICML*, pages 7404–7413, 2019.

[120] Y. Zhang, Z. Qiu, T. Yao, C.-W. Ngo, D. Liu, and T. Mei. Transferring and regularizing prediction for semantic segmentation. In *Proc. CVPR*, pages 9621–9630, 2020.

[121] Z. Zheng and Y. Yang. Rectifying pseudo label learning via uncertainty estimation for domain adaptive semantic segmentation. *International Journal of Computer Vision*, 129(4):1106–1120, 2021.

[122] X. Zhu, H. Zhou, C. Yang, J. Shi, and D. Lin. Penalizing top performers: Conservative loss for semantic segmentation adaptation. In *Proc. ECCV*, pages 568–583, 2018.

[123] Y. Zou, Z. Yu, X. Liu, B. Kumar, and J. Wang. Confidence regularized self-training. In *Proc. ICCV*, pages 5982–5991, 2019.

[124] Y. Zou, Z. Yu, B. Vijaya Kumar, and J. Wang. Unsupervised domain adaptation for semantic segmentation via class-balanced self-training. In *Proc. ECCV*, pages 289–305, 2018.

Yuxi Wang received the Bachelor degree from North Eastern University, China, in 2016, and the PhD degree from University of Chinese Academy of Sciences (UCAS), Institute of Automation, Chinese Academy of Sciences (CASIA), in January 2022. He is now an assistant professor in the Center for Artificial Intelligence and Robotics (CAIR), Hong Kong Institute of Science & Innovation, Chinese Academy of Science (HKISI-CAS). His research interests include transfer learning, domain adaptation and



computer vision.



Jian Liang received the B.E. degree in Electronic Information and Technology from Xi'an Jiaotong University and Ph.D. degree in Pattern Recognition and Intelligent Systems from NLPR, CASIA in July 2013, and January 2019, respectively. He was a research fellow at National University of Singapore from June 2019 to April 2021. Now he joins NLPR as an associate professor. His research interests focus on transfer learning, pattern recognition, and computer vision.



Zhaoxiang Zhang Zhaoxiang Zhang received his bachelor's degree from the Department of Electronic Science and Technology in the University of Science and Technology of China (USTC) in 2004. After that, he was a Ph.D. candidate under the supervision of Professor Tieniu Tan in the National Laboratory of Pattern Recognition, Institute of Automation, Chinese Academy of Sciences, where he received his Ph.D. degree in 2009. In October 2009, he joined the School of Computer Science and Engineering, Beihang

University, as an Assistant Professor (2009-2011), an Associate Professor (2012-2015) and the Vice-Director of the Department of Computer application technology (2014-2015). In July 2015, he returned to the Institute of Automation, Chinese Academy of Sciences. He is now a full Professor in the Center for Research on Intelligent Perception and Computing (CRIPAC) and the National Laboratory of Pattern Recognition (NLPR). His research interests include Computer Vision, Pattern Recognition, and Machine Learning. Recently, he specifically focuses on deep learning models, biologically-inspired visual computing and human-like learning, and their applications on human analysis and scene understanding. He has published more than 200 papers in international journals and conferences, including reputable international journals such as JMLR, IEEE TIP, IEEE TNN, IEEE TCSVT, IEEE TIFS and top level international conferences like CVPR, ICCV, NIPS, ECCV, AAAI, IJCAI and ACM MM. He is serving or has served as the Associated Editor of IEEE T-CSVT, Pattern Recognition, Neurocomputing, and Frontiers of Computer Science. He has served as the Area Chair, Senior PC of international conferences like CVPR, NIPS, ICML, AAAI, IJCAI and ACM MM. He is a Senior Member of IEEE, a Distinguished Member of CCF, and a Distinguished member of CAAI.